PROCEEDINGS

of the

TENTH WORLD CONFERENCE on EARTHQUAKE ENGINEERING

19-24 July 1992
Madrid
Spain

OFFPRINT

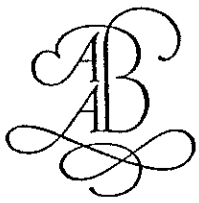

Published by
A.A.Balkema / Rotterdam / Brookfield / 1992

Earthquake Engineering, Tenth World Conference © 1992 Balkema, Rotterdam. ISBN 90 5410 060 5

Seismic response of sheet pile walls

W.D. Liam Finn & Guoxi Wu
Department of Civil Engineering, University of British Columbia, Vancouver, B.C., Canada

N. Yoshida
Sato Kogyo Co. Ltd. Tokyo, Japan & University of British Columbia, Vancouver, B.C., Canada

ABSTRACT: A nonlinear effective stress method for the seismic response analysis of sheet pile walls is validated using data from centrifuge tests on a model wall with dry backfill. The method is then applied to estimate bending moments and displacements when the backfill is saturated. The moments and displacements are highly dependent on the level of porewater pressure developed during shaking. The application of the widely used Mononobe-Okabe pseudo-static approach appears to overestimate the peak moments at high levels of shaking.

1 INTRODUCTION

Seismic design of earth retaining structures is usually based on seismic forces and pressures estimated by the Mononobe-Okabe method of analysis (Okabe, 1926; Mononobe and Matsuo, 1929). The method is based on a modification of Coulomb's classical earth pressure theory for dry sands to account for the inertial forces corresponding to uniform horizontal and vertical accelerations, $k_h g$ and $k_v g$, respectively. The magnitudes of the seismic coefficients k_h and k_v are based on local or regional experience of earthquake damage to retaining structures.

The Mononobe-Okabe method has been validated for dry sands by both shaking table (Sherif et al., 1982; Sherif and Fang, 1984) and centrifuge tests (Steedman, 1984).

The tests by Sherif are particularly interesting because during shaking the walls were rotated outwards to allow the mobilization of the full shearing resistance of the fill behind the wall and the distribution of accelerations throughout the fill was essentially constant. Therefore the basic assumptions of the theory were satisfied. In these tests, values of the active pressure seismic coefficient K_{AE} derived from the test data agreed very closely with values computed using the Mononobe-Okabe expression for K_{AE} applicable to a vertical wall with horizontal backfill.

In the case of a vertical wall retaining a horizontal backfill, the dynamic active earth pressure coefficient, K_{AE}, is given by

$$K_{AE} = \frac{\cos^2(\phi-\psi)}{\cos\psi\cos(\psi+\delta)\left[1+\sqrt{\frac{\sin(\phi+\delta)\sin(\phi-\psi)}{\cos(\delta+\psi)}}\right]^2} \quad (1)$$

where ϕ is the soil friction angle, δ is the wall friction angle, and ψ, the seismic inertia angle, is given by

$$\psi = \tan^{-1}\left[\frac{k_h}{(1-k_v)}\right] \quad (2)$$

The seismic inertia angle represents the angle through which the resultant of the gravity force and the inertial forces is rotated from vertical. The Mononobe-Okabe relationship for P_{AE} for dry backfills is equal to

$$P_{AE} = K_{AE}\,\frac{1}{2}\,[\gamma_d\,(1-k_v)]\,H^2 \quad (3)$$

and acts at an angle δ from the normal to the back of the wall of height H.

The location of the active pressure force P_{AE} is generally higher than one-third of the height of the wall (H/3) above the base of the wall. Sherif and his colleagues found the resultant reached a height of 0.45 ft in their tests. The Mononobe-Okabe theory gives no guidance on the nature of the pressure distribution so that the location of the active and passive forces during an earthquake are somewhat uncertain.

The Mononobe-Okabe method is also routinely applied to cases not complying with the basic assumptions of the method. The most common and important cases are when the backfill is saturated and the displacements of the wall do not meet the conditions for a Coulomb type of analysis. The classical case embodying both of these exceptions is the anchored sheet pile wall.

The seismic response of these walls is being studied at the University of British Columbia using dynamic effective stress finite element analysis and data from centrifuge tests conducted on the large geotechnical centrifuge at Cambridge (Steedman, 1984; Steedman and Zeng, 1990). This paper presents preliminary findings from this study.

2 METHOD OF ANALYSIS

The dynamic response analyses were computed using the computer program TARA-3 (Finn et al., 1986; Finn, 1985). The program incorporates a method for nonlinear dynamic effective stress analysis. The response in shear is assumed to be nonlinear and hysteretic. The response to changes in all-round pressure, defined by the bulk modulus, is assumed to be nonlinear and dependent on the mean normal effective stress. In effect hysteresis under hydrostatic pressure is neglected in comparison with the pronounced hysteretic response in shear. Residual porewater pressures in saturated soils are computed using the Martin-Finn-Seed (1975) porewater pressure model, modified to include the effects of any initial static shear stresses. TARA-3 conducts both static and dynamic finite element analyses.

Dynamic analysis starts from the static stress-strain condition in each finite element. This procedure gives the most realistic representation of subsequent permanent deformations. Dynamic analysis in engineering practice usually ignores the initial static strain conditions and starts from the origin of the stress-strain curve in all elements, even in those which carry high shear stresses.

3 VALIDATION OF ANALYSIS

The first step is to check how well the program can simulate the dynamic and residual moments and deformations in the sheet pile wall for the simplest case of the cantilever wall using centrifuge test data from a model wall (Steedman, 1984).

3.1 Model test

The model of the cantilever wall is shown in Figure 1. The wall is bolted to the floor of the centrifuge model container. The height of the wall is 78 mm and it has a thickness of 2.04 mm. When tested at a nominal centrifuge acceleration of 90 g, the model corresponds to a prototype wall 7.0 m high and 184 mm thick. The elastic modulus $E = 6.4 \times 10^7$ kN/m^2, the cross-sectional area $A = 0.184$ m^2, and moment of inertia $I = 5.2 \times 10^{-4}$ m^4/m run.

The wall is backfilled with dry Leighton-Buzzard sand, 14/25, poured to a void ratio $e = 0.51$ corresponding to a relative density $D_r = 96\%$. The effective angle of internal friction, $\phi' = 40°$ and the unit weight is $\gamma_d = 18.8$ kN/m^3.

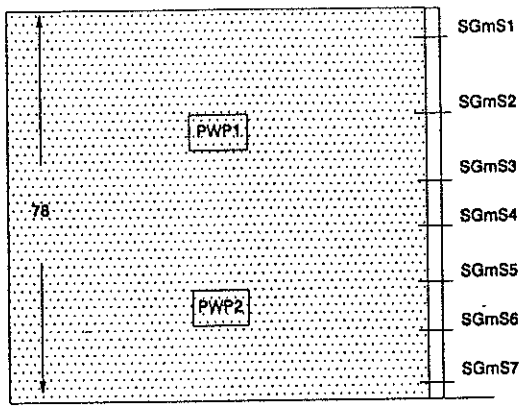

Figure 1. Instrumented model cantilever wall.

The peak input acceleration is 42.7% of gravity acceleration and the duration at prototype scale is 12s. The input is predominantly sinusoidal with varying amplitude and has a dominant frequency of 1.42 Hertz at prototype scale. This is the scale at which the calculations are carried out.

The accelerations were recorded near the top of the wall at SGmS1. Displacements of the wall were measured at the top of the wall. Full bridge strain gauge circuits were used to record the dynamic and residual bending moments at seven locations along the height of the wall from SGmS1 to SGmS7.

3.2 Finite element analysis

The finite element mesh for the cantilever retaining wall is shown in Figure 2. Beam elements were used to model the wall. The mesh comprises 127 finite elements and 140 nodes.

Figure 2: Finite element mesh of the cantilever wall.

A static analysis of wall and backfill was first conducted to establish the stress-strain field prior to earthquake excitation. The program simulated the gradual construction process of the model.

3.3 Measured and Computed Responses

Computed and measured bending moments are shown in Figure 3 for location SGmS7, where the bending moments are greatest. The agreement between measured and computed dynamic and residual moments is very close. The residual bending moments reflect the permanent deformations imposed on the wall by the backfill due to its nonlinear hysteretic response. The close agreement between measured and computed residual moments indicates that the analysis is properly simulating the response of the backfill.

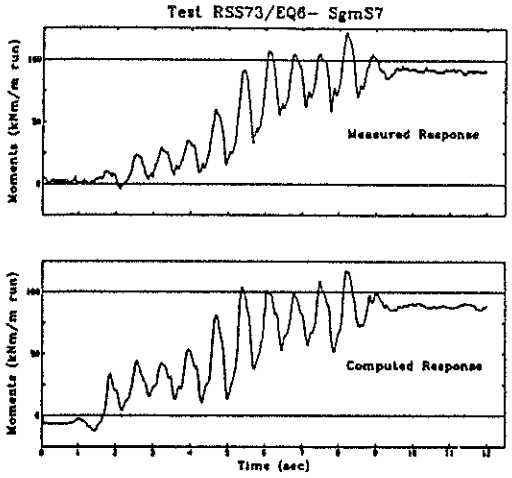

Figure 3: Measured and computed bending moments at SGmS7.

The measured and computed displacements at the top of the wall are shown in Figure 4. The agreement appears satisfactory for engineering purposes. The agreement further down the wall near SGmS4 is very good. A digitized record was not available for this record but the peak dynamic and permanent deformation can be read from the output and are given in Table 1.

On the basis of these data, TARA-3 appears to simulate the seismic response of the wall with an accuracy adequate for engineering purposes.

4 SUBMERGED BACKFILL: DYNAMIC ANALYSIS

To investigate the behaviour of saturated backfill, dynamic response analyses were conducted on

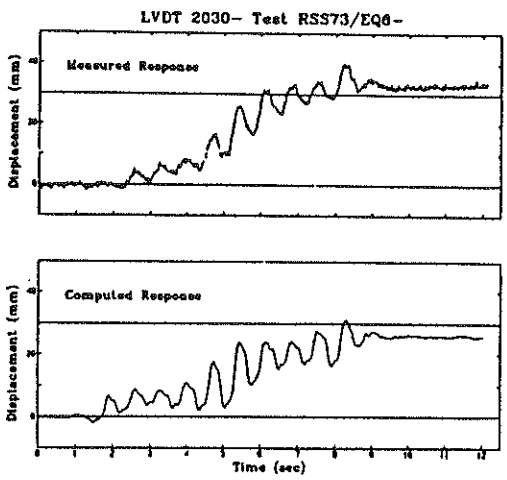

Figure 4: Measured and computed displacements at top of wall.

Table 1. Comparison of maximum and residual displacements of cantilever wall at prototype scale in mm.

Transducer Location	Max. Displ.		Residual Displ.	
	Meas.	Comp.	Meas.	Comp.
SGm S4	11.8	10.0	9.0	8.0
Top of wall	40.3	31.3	33.0	26.0

some prototype wall using TARA-3. The backfill was assumed to be fully saturated over its entire depth. Three cases were considered. First is the case where the backfill does not develop any significant porewater pressures during shaking. This corresponds to a total stress nonlinear analysis using properties based on the initial effective stress regime.

Then effective stress dynamic analyses were conducted in which porewater pressures were generated during the analysis at rates leading to average porewater pressure ratios, u/σ_{vo}', of 40% and 60% where u = seismic porewater pressure and σ_{vo}' = initial vertical effective stress. A typical porewater pressure development curve is given in Figure 5.

The distribution of the dynamic increments in moment along the wall are given in Table 2. There is a steady increase in bending moments with increasing porewater pressures. The peak moment at SGmS7 doubles over the range in porewater pressures analyzed. The moment distributions are plotted in Figure 6. The time histories of the dynamic moments at location SGmS7 near the

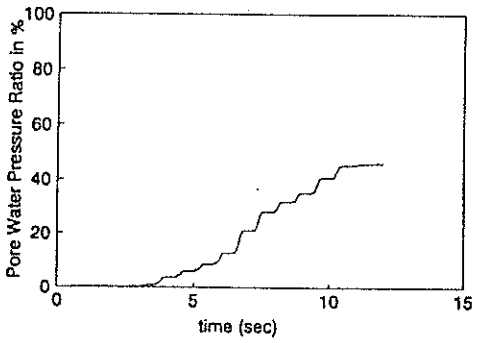

Figure 5: Development of porewater pressures during earthquake shaking.

Table 2. Dynamic moment increments for various porewater pressure ratios in saturated backfill.

Peak Moments	Pore Pressure Ratio (%) 0%	40%	60%
SGm S1	4	5	6
SGm S2	30	39	47
SGm S3	65	87	102
SGm S4	69	112	142
SGm S5	99	176	224
SGm S6	170	290	360
SGm S7	243	400	490

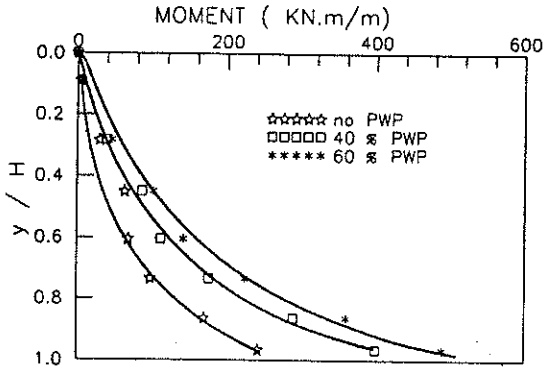

Figure 6: Peak dynamic moments for porewater pressure ratios of 0%, 40%, and 60% in the saturated backfill.

bottom of the wall for the three levels of porewater pressure are given in Figure 7. The substantial residual moments may also be read from Figure 7.

The time histories of displacements are given in Figure 8 from which the residual displacements at the end of the earthquake may also be obtained. It

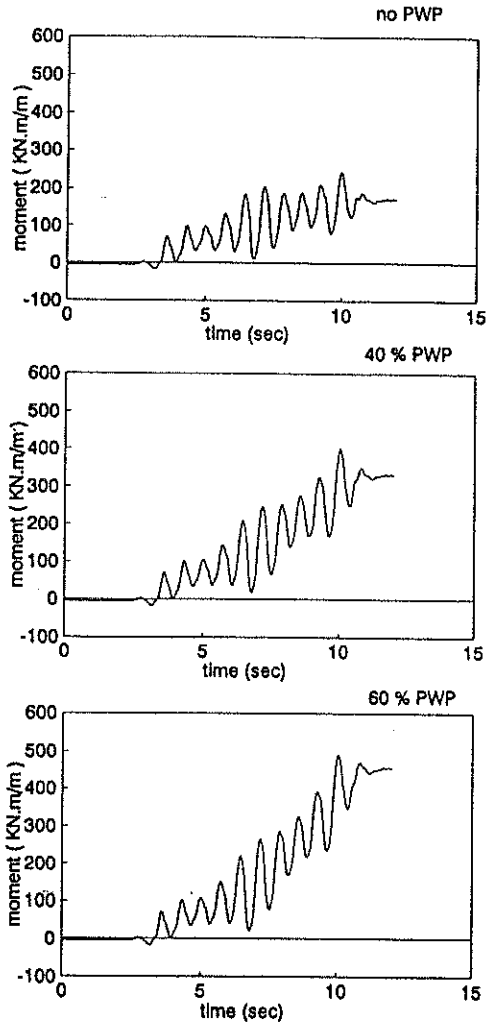

Figure 7: Distribution of dynamic moments in wall for porewater pressure ratios of 0%, 40%, and 60% in the saturated backfill.

may be seen that both the cyclic and permanent displacements increase with increasing porewater pressures in the backfill.

The acceleration response at SGmS1 near the top of the wall is shown in Figure 9 and reflects the sinusoidal nature of the input motions.

5 SUBMERGED BACKFILL: MONONOBE-OKABE

Common practice in the application of Mononobe-Okabe to submerged backfills follows the procedures described by Matsuzawa et al. (1985). They recognize two limiting cases; restrained water in which the water moves with the soil grains which is suitable for low permeability

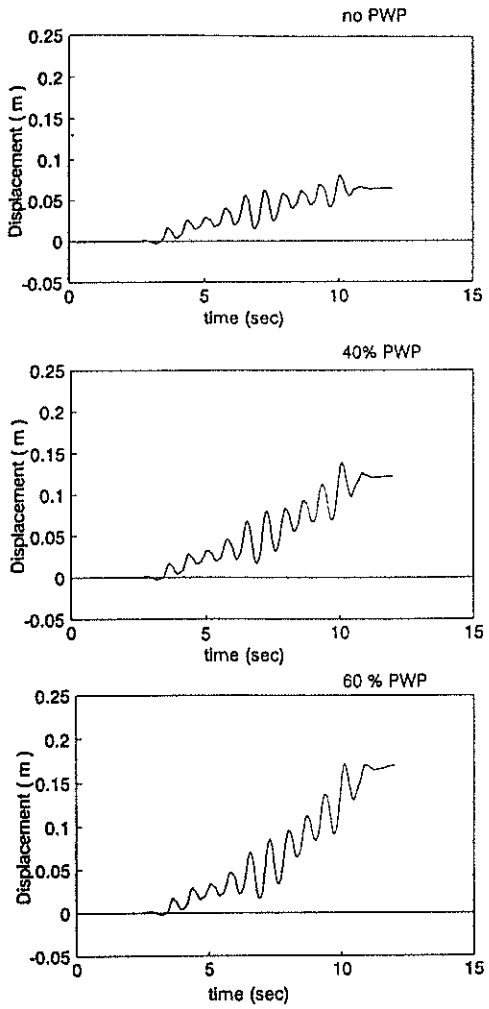

Figure 8: Wall top displacements for porewater pressure ratios of 0%, 40%, and 60% in the saturated backfill.

soils and free water in which the effects of soil and water are considered separately. This latter procedure is considered suitable for very free draining soils. Judgement is required for intermediate conditions.

5.1 Restrained water case

Here Matsuzawa et al. (1985) make the assumption that pore pressures do not change as a result of horizontal accelerations. Considering a Coulomb wedge and subtracting the static pore pressures, there is a horizontal inertia force proportional to $\gamma_t \cdot k_h$ and a vertical force proportional to γ_b. Thus, in the absence of vertical accelerations, the equivalent seismic angle is:

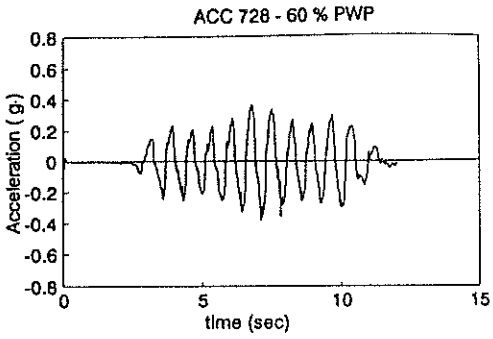

Figure 9: Acceleration at top of wall when porewater pressure ratio is 60%.

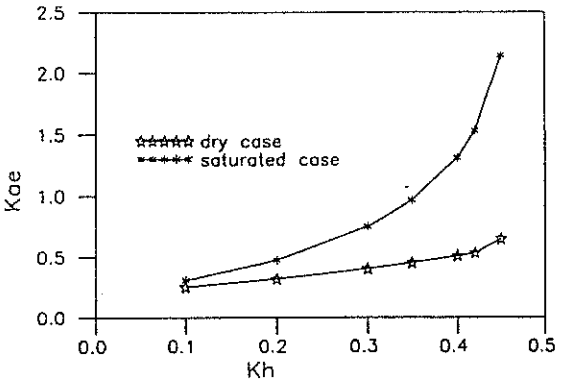

Figure 10: Effect of saturation on the active seismic pressure coefficient K_{AE}.

$$\psi_e = \tan^{-1} \frac{\gamma_t \cdot k_h}{\gamma_b} \quad (4)$$

That is, the equivalent horizontal seismic coefficient is:

$$k_{he} = \frac{\gamma_t}{\gamma_b} k_h \quad (5)$$

The variation of k_{he} with level of shaking is shown in Figure 10. Clearly, in this method, the effects of submergence increase rapidly with increasing level of shaking.

Using k_{he} in the Mononobe-Okabe theory together with a unit weight γ_b will give P_{AE}, to which the static water pressures must be added.

If vertical accelerations are present, Matsuzawa et al. (1985) recommend using:

$$\psi_e = \tan^{-1} \left[\frac{\gamma_t \cdot k_h}{\gamma_b (1-k_v)} \right] \quad (6)$$

When this procedure is applied to the

prototype wall with $\delta = \phi/2$, the peak dynamic moment increment at SGmS7 is 760 kNm/m which is much greater than the peak moment by finite element analysis even at 60% porewater pressure.

5.2 Free water case

Matsuzawa et al. (1985) suggest that the total active thrust is made up of:

1) A thrust from the mineral skeleton, computer using:

$$k_{he} = \frac{\gamma_d}{\gamma_b} k_h = \frac{G_s}{G_s - 1} k_h \quad (7)$$

and

$$\psi_e = \tan^{-1}\left[\frac{k_{he}}{(1-k_v)}\right] \quad (8)$$

where γ_d is the dry unit weight, and G_s is the specific gravity of the solids. A unit weight of γ_b is used in the equation for P_{AE}.

2) The hydrodynamic water pressure force for the free water within the backfill, P_{wd}, is given by the Westergaard (1933) relationship

$$P_{wd} = \frac{7}{12} \cdot k_h \cdot \gamma_w H^2 \quad (9)$$

and acts at 0.4 H above the base of the wall.

The peak dynamic moment at SGmS7 for this assumption is 800 kNm/m, which is comparable to the moment (760 kNm/m) calculated using the restrained water concept. The peak moment for a fully fluidized backfill is only 633 kNm/m. The dynamic moment increments were calculated by subtracting the moments due to static active pressures from the total Mononobe-Okabe moments. The latter moments are lower bound because they were calculated assuming the resultant seismic force acted 0.33H above the base of the wall. The actual location may vary up to about 0.45 H. The contribution of the mass of the wall to the bending moment is not included in the Mononobe-Okabe calculations.

6 CONCLUSIONS

There are large differences between the peak dynamic moments in sheet pile walls with saturated backfills under very strong shaking estimated by the Mononobe-Okabe method and finite element analysis. The Mononobe-Okabe method would appear to be very conservative. It gives the same peak moments irrespective of the level of pore pressures developed in the backfill. One would expect the moments to vary with the level of porewater pressure. These conclusions are tentative and more detailed studies are being carried out.

ACKNOWLEDGEMENTS

This research was supported by the National Science and Engineering Council of Canada.

REFERENCES

Finn, W.D. Liam 1985. Dynamic effective stress response of soil structures: theory and centrifugal model studies. Proc., 5th Int. Conf. on Num. Methods in Geomech., Nagoya, Japan, 1: 35-36.

Finn, W.D. Liam, M. Yogendrakumar, N. Yoshida and H. Yoshida 1986. TARA-3: A program to compute the response of 2-D embankments and soil-structure interaction systems to seismic loading. Dept. of Civil Engineering, University of British Columbia, Vancouver, B.C., Canada.

Martin, G.R., W.D. Liam Finn & H.B. Seed 1975. Fundamentals of liquefaction under cyclic loading. Proc. Paper 11284, J. Geotech. Eng. Div., ASCE 101:5, 324-438.

Matsuzawa, H., I. Ishibashi & M. Kawamura 1985. Dynamic soil and water pressures of submerged soils. ASCE, Journal of Geotechnical Engineering, 111:10, 1161-1176.

Mononobe, N. & M. Matsuo 1929. On the determination of earth pressures during earthquakes. Proc. World Engineering Congress, 9.

Okabe, S. 1926. General theory of earth pressures. Journal, Japan Soc. of Civil Engrs., 12:1.

Sherif, M.A., I. Ishibashi & C.D. Lee 1982. Earth pressure against rigid retaining walls. J. of the Geot. Eng. Div., ASCE, 108:5, 679-695.

Sherif, M.A. & Y.S. Fang 1984. Dynamic earth pressures on walls rotating about the top, Soils and Foundations. 24:4, 109-117.

Steedman, R.S. 1984. Modelling the behaviour of retaining walls in earthquakes. Ph.D. Thesis, Engineering Dept., Cambridge University, UK.

Steedman, R.S. & X. Zeng, 1990. The influence of phase on the calculation of pseudo-static earth pressure on a retaining wall. Geotechnique 40:1, 103-112.

Westergaard, H.M. 1933. Water pressures on dams during earthquakes. Transactions, ASCE 98: 418-472.